Role of linear and cubic terms for drift-induced Dresselhaus spin-orbit splitting in a two-dimensional electron gas

M. Studer,[1,2] M. P. Walser,[1,2] S. Baer,[2] H. Rusterholz,[3] S. Schön,[3] D. Schuh,[4] W. Wegscheider,[2] K. Ensslin,[2] and G. Salis[1,*]

[1]*IBM Research-Zurich, Säumerstrasse 4, 8803 Rüschlikon, Switzerland*

[2]*Solid State Physics Laboratory, ETH Zurich, 8093 Zurich, Switzerland*

[3]*FIRST Center for Micro- and Nanosciences, ETH Zurich, 8093 Zurich, Switzerland*

[4]*Institut für Experimentelle und Angewandte Physik, Universität Regensburg, 93040 Regensburg, Germany*

(Received 28 September 2010; published 17 December 2010)

The Dresselhaus spin-orbit interaction (SOI) of a series of two-dimensional electron gases hosted in GaAs/AlGaAs and InGaAs/GaAs (001) quantum wells (QWs) is measured by monitoring the precession frequency of the spins as a function of an in-plane electric field. The measured spin-orbit-induced spin splitting is linear in the drift velocity, even in the regime where the cubic Dresselhaus SOI is important. We relate the measured splitting to the Dresselhaus coupling parameter γ, the QW confinement, the Fermi wave number k_F, and strain effects. From this, γ is determined quantitatively, including its sign.

DOI: 10.1103/PhysRevB.82.235320 PACS number(s): 73.21.Fg, 85.75.−d, 71.70.Ej, 78.47.−p

The spin-orbit interaction (SOI) couples electron spins to the orbital motion. In semiconductor quantum structures, SOI often limits the spin lifetime and therefore needs to be minimized when spins are to be used for processing or storing information. On the other hand, SOI has the potential to locally control spins by electrical means.[1] The reliable manipulation of spins is crucial for spin-based quantum computing[2] and for spintronic applications.[3] For a two-dimensional electron gas (2DEG) hosted in a semiconductor with zinc-blende structure, there are two main sources for SOI: the Rashba SOI (Ref. 4) and the Dresselhaus SOI.[5] The Dresselhaus SOI is a bulk property as it arises form the inversion asymmetry of the crystal. The resulting spin splitting is cubic in the components of the electron wave vector $\mathbf{k}=(k_x,k_y,k_z)$. In a 2DEG, the quantum confinement along the growth direction z leads to bound states with the expectation value $\langle k_z\rangle=0$ and a quantized value for $\langle k_z^2\rangle$. This constriction of the orbital motion modifies the spin splitting in terms of the in-plane momentum components: in addition to a cubic dependence, there is also a term proportional to $\langle k_z^2\rangle$ that is linear in the components of the in-plane wave vector $\mathbf{k}=(k_x,k_y)$.[6] The strength of both terms is given by the Dresselhaus coupling constant γ. The value of γ has been measured quantitatively with various techniques, including Raman scattering,[7] magnetotransport,[8–10] spin-dephasing measurements,[11] and spin-grating measurements.[12] These techniques probe $\mathbf{k}$ states selectively at the Fermi surface, and the spin splitting is directly related to the Fermi wave number k_F. In contrast, drift-related experiments[13–17] involve a small displacement $\delta\mathbf{k}$ of the Fermi surface and lead to a drift-induced spin splitting that is proportional to $\delta k \ll k_F$ and a direction dependence that can be described by an effective magnetic field $\mathbf{B}_{df}(\delta\mathbf{k})$. This field is composed of a Rashba component $\mathbf{B}_{df,R}$ and a Dresselhaus component $\mathbf{B}_{df,D}$, which have different symmetry with respect to $\delta\mathbf{k}$. Quantitative values, including the absolute sign, for both Rashba and Dresselhaus SOI can be obtained by monitoring the coherent spin precession in an external magnetic field $\mathbf{B}_{ext}$.[14–16]

In this work, we investigate the interplay of the linear and cubic terms of the Dresselhaus SOI of a 2DEG as manifested in measurements of $\mathbf{B}_{df,D}$ versus $\delta\mathbf{k}$. The cubic term becomes important for $k_F^2 > \langle k_z^2\rangle$, and it has been suggested that in this regime $\mathbf{B}_{df,D}$ has a cubic dependence on $\delta\mathbf{k}$.[15,18–20] Here we show that $\mathbf{B}_{df,D}$ depends linearly on δk ($\ll k_F$), even in the regime of $k_F^2 \gg \langle k_z^2\rangle$. A central aspect of this work is to discuss how the linear and the cubic Dresselhaus SOI terms contribute to $\mathbf{B}_{df,D}$ by deriving an explicit expression for $\mathbf{B}_{df,D}(\delta\mathbf{k})$ from the Dresselhaus Hamiltonian H_D. The calculations show that the slope of $B_{df,D}$ versus δk is decreased by the cubic term, and changes its sign when $k_F^2 > 2\langle k_z^2\rangle$. We experimentally studied samples made of two material systems displaying different Fermi and confinement energies, namely, 10-nm-wide and 20-nm-wide InGaAs/GaAs quantum wells (QWs), and 15-nm-wide GaAs/AlGaAs QWs. A linear dependence of $B_{df,D}$ on δk is measured in all cases of $\langle k_z^2\rangle/k_F^2$. Cubic contributions are small for the GaAs/AlGaAs QWs and we find $\gamma \approx -6$ eV Å^3. For the InGaAs/GaAs QWs, cubic contributions significantly modify the slope of $B_{df,D}$ versus δk. In addition, a more detailed analysis of the slope provides evidence of a strain-induced contribution that has the same symmetry as the linear Dresselhaus SOI.

The paper is organized as follows: first we lay out the theoretical framework and define the Dresselhaus SOI and the coordinate system, the basis for an unambiguous definition of the sign of γ. Then, we derive the linear dependence of B_{df} versus δk. Next, we present experimental data for a series of samples in which the importance of the cubic term varies, and finally discuss the results with respect to the theory developed.

I. DRESSELHAUS SPIN SPLITTING

Dresselhaus SOI for a 2DEG is described here in the coordinate system (x,y,z) defined by the cubic crystallographic axes [100], [010], and [001]. These directions are specified in a GaAs primitive cell, with the cation (Ga) residing at (0, 0, 0) and the anion (As) located at $(\frac{1}{4},\frac{1}{4},\frac{1}{4})$. This is the same convention as used by wafer manufacturers and is compatible with the literature on direction-selective etching processes.[21,22] In contrast, in some theoretical works,[23,24] the anion is placed at the origin of the coordinate system. This specification is important for an unambiguous definition of

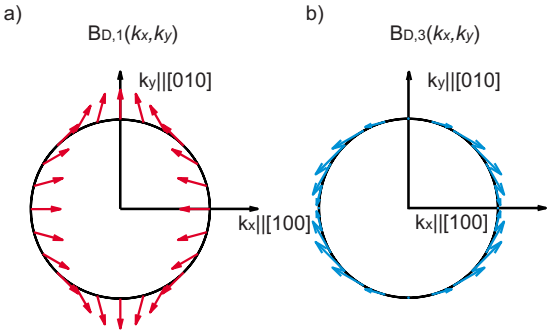

FIG. 1. (Color online) Symmetry of the effective magnetic field resulting from Dresselhaus SOI: (a) linear term $\mathbf{B}_{\mathrm{D},1}$ and (b) cubic term $\mathbf{B}_{\mathrm{D},3}$ (we assume $g<0$ and $\gamma<0$).

the Dresselhaus parameter γ because the exchange of cation and anion involves a change in the sign of γ.[23] In the following, we discuss (001)-grown QWs with one occupied subband and the Dresselhaus Hamiltonian:

$$H_{\mathrm{D}} = \gamma[-\langle k_z^2\rangle(k_x\sigma_x - k_y\sigma_y) + (k_y^2 k_x\sigma_x - k_x^2 k_y\sigma_y)], \qquad (1)$$

where $\langle k_z^2\rangle$ is the quantum-mechanical expectation value of k_z^2 with respect to the envelope wave function of the occupied subband and $\vec{\sigma}=(\sigma_x,\sigma_y,\sigma_z)$ are the Pauli matrices. In this notation, two terms show up: a term that is linear in the in-plane momentum components and a term that is cubic. To study the interplay of these two terms, we compare their magnitude for $\mathbf{k}=(k_x,k_y)$ on the Fermi surface, i.e., for $k_x^2+k_y^2=k_{\mathrm{F}}^2$: the ratios $k_x^2/\langle k_z^2\rangle$ and $k_y^2/\langle k_z^2\rangle$ have an upper limit of $k_{\mathrm{F}}^2/\langle k_z^2\rangle$ and are zero for certain orientations of $\mathbf{k}$. Therefore, the linear term is dominant in the case of strong confinement, i.e., for $\langle k_z^2\rangle \gg k_{\mathrm{F}}^2$. In terms of the QW sheet density n_s and the QW width w, the importance of cubic terms scales with the product $n_s w^2$ because $k_{\mathrm{F}}^2=2\pi n_s$ and $\langle k_z^2\rangle \propto (\pi/w)^2$.

For the further discussion, it is convenient to express H_{D} as a spin splitting induced by an effective magnetic field $\mathbf{B}_{\mathrm{D}}$ that depends on the electron wave vector $\mathbf{k}$,

$$E(\mathbf{k},\uparrow) - E(\mathbf{k},\downarrow) = g\mu_B|\mathbf{B}_{\mathrm{D}}(\mathbf{k})|. \qquad (2)$$

Here $\mu_B=|e|\hbar/2m_0$ is Bohr's magneton of the free electron with mass m_0, and g is the effective g factor in the semiconductor QW. $E(\mathbf{k},\uparrow)$ and $E(\mathbf{k},\downarrow)$ are the two eigenvalues of H_{D} for a given $\mathbf{k}$. In our coordinate system and in correspondence with Eq. (1), we separate the linear and cubic contributions according to

$$\mathbf{B}_{\mathrm{D}}(k_x,k_y) = \mathbf{B}_{\mathrm{D},1}(k_x,k_y) + \mathbf{B}_{\mathrm{D},3}(k_x,k_y), \qquad (3)$$

$$\mathbf{B}_{\mathrm{D},1}(k_x,k_y) = \frac{-2\gamma\langle k_z^2\rangle}{g\mu_B}\begin{pmatrix} k_x \\ -k_y \end{pmatrix}, \qquad (4)$$

$$\mathbf{B}_{\mathrm{D},3}(k_x,k_y) = \frac{2\gamma}{g\mu_B}\begin{pmatrix} k_x k_y^2 \\ -k_y k_x^2 \end{pmatrix}. \qquad (5)$$

The different symmetries of the two contributions are illustrated in Fig. 1 by plotting the vector fields $\mathbf{B}_{\mathrm{D},1}(k_x,k_y)$ and $\mathbf{B}_{\mathrm{D},3}(k_x,k_y)$ for a specific $|\mathbf{k}|$. The magnitude of $\mathbf{B}_{\mathrm{D},1}$ does not depend on the direction of $\mathbf{k}$, whereas $\mathbf{B}_{\mathrm{D},3}$ is maximal for $\mathbf{k}$ along the [110] and [1$\bar{1}$0] directions, and zero along [100] and [010].

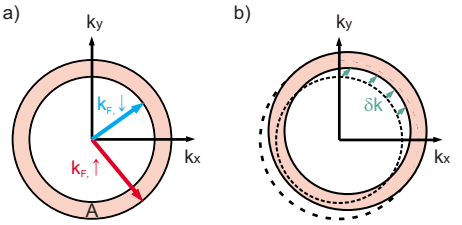

FIG. 2. (Color online) (a) 2DEG with finite spin polarization: two Fermi circles with radii $k_{\mathrm{F},\uparrow}$ and $k_{\mathrm{F},\downarrow}$ limit the spin-polarized k-space area $A=\pi(k_{\mathrm{F},\uparrow}^2-k_{\mathrm{F},\downarrow}^2)$ [shaded]. (b) Spin-polarized 2DEG in an in-plane electric field: the Fermi circles and the area A are shifted by a drift wave vector $\delta\mathbf{k}$.

So far, we have only considered Dresselhaus SOI. Other sources of SOI include structure inversion asymmetry (Rashba SOI) and strain. Their corresponding spin splitting can also be expressed as an effective magnetic field. In case of the Rashba SOI, this field can be separated from the Dresselhaus SOI because of its different symmetry in $\mathbf{k}$. However, biaxial strain gives rise to a spin splitting that has the same symmetry as the linear Dresselhaus SOI [first term in Eq. (1)]. Its effective magnetic field can be expressed as[20,25]

$$\mathbf{B}_{\mathrm{S}}(k_x,k_y) = \frac{2\beta_S}{g\mu_B}\begin{pmatrix} k_x \\ -k_y \end{pmatrix}. \qquad (6)$$

Here, $\beta_S=D(\epsilon_{zz}-\epsilon_{xx})$, where D is a material parameter and ϵ_{ij} is the strain tensor. Such a component has been observed in InGaAs epilayers grown on GaAs, where it can be stronger than the Dresselhaus contribution.[14] There is no systematic work describing the strain contribution in n-doped QWs and only few experimental studies.[26] For completeness and cross referencing, we introduce the Rashba coupling constant α and the effective magnetic field induced by Rashba SOI,

$$\mathbf{B}_{\mathrm{R}} = \frac{2\alpha}{g\mu_B}\begin{pmatrix} k_y \\ -k_x \end{pmatrix}. \qquad (7)$$

II. CALCULATION OF THE DRIFT-INDUCED SPIN SPLITTING

The effective magnetic field $\mathbf{B}_{\mathrm{D}}(\mathbf{k})$ discussed in the previous section affects individual electron spins. Drift-related experiments involve all states near the Fermi surface, and a corresponding average of $\mathbf{B}_{\mathrm{D}}(\mathbf{k})$ is observed. In our experiment, only a part of the 2DEG is spin polarized, and we measure the coherent precession of those spins in their corresponding field $\mathbf{B}_{\mathrm{D}}(\mathbf{k})$. The initial spin polarization is oriented along $\mathbf{z}\equiv[001]$ (denoted as "spin-up" polarization), and can be described by two Fermi wave numbers $k_{\mathrm{F},\uparrow}$ and $k_{\mathrm{F},\downarrow}$: spin-up (spin-down) states are homogeneously filled up to $k_{\mathrm{F},\uparrow}$ ($k_{\mathrm{F},\downarrow}$) at 0 K [Fig. 2(a)]. The spin polarization is given as $(k_{\mathrm{F},\uparrow}^2-k_{\mathrm{F},\downarrow}^2)/2\pi n_s$.

To connect $\mathbf{B}_{\mathrm{D}}(\mathbf{k})$ with the spin-precession frequency measured in the experiment, we average $\mathbf{B}_{\mathrm{D}}(\mathbf{k})$ over the spin-

TABLE I. Overview of all samples: QW material, structure, width w, and expected $\langle k_z^2\rangle$ (calculated); n_s and k_F^2 are experimental results from Hall measurements, and μ is deduced from the four-terminal resistance. The Dresselhaus drift parameter β^* is determined from the drift-induced change in the spin-precession frequency, using TRFR (samples 1 and 2) and TRKR (samples 3–5). γ is calculated from β^*, $\langle k_z^2\rangle$, and k_F^2. For samples 1 and 2 the calculation of γ in addition assumes the same $\beta_S \approx 7\times 10^{-14}$ eV m. β is the linear term of the Dresselhaus SOI and calculated using $\beta=-\gamma\langle k_z^2\rangle$. All data in this table has been obtained at a temperature of 40 K.

No.	QW/host material (number of wells)	w (nm)	μ (m^2/V s)	$\langle k_z^2\rangle\times 10^{16}$ (m^{-2})	$k_F^2\times 10^{16}$ (m^{-2})	$n_s\times 10^{15}$ (m^{-2})	$\beta^*\times 10^{-13}$ (eV m)	$\gamma\times 10^{-30}$ (eV m^3)	$\beta\times 10^{-13}$ (eV m)
1	$In_{.10}Ga_{.90}As/GaAs$ (1×)	20	1.3	0.95	3.2	5.2	0.2	−7.5	0.7
2	$In_{.12}Ga_{.88}As/GaAs$ (1×)	10	4.5	2.25	2.8	4.5	1.3	−7.5	1.7
3	$GaAs/Al_{.3}Ga_{.7}As$ (14×)	15	51	2.5	0.74	1.2	1.7	−8.0	2.0
4	$GaAs/Al_{.3}Ga_{.7}As$ (14×)	15	36	2.5	0.86	1.4	1.0	−4.7	1.2
5	$GaAs/Al_{.3}Ga_{.7}As$ (14×)	15	24	2.5	0.99	1.6	1.0	−5	1.3

polarized area $A=\pi(k_{F,\uparrow}^2-k_{F,\downarrow}^2)$ [shaded in Fig. 2(a)]. This approach is reasonable for nonselective optical probe techniques and for fast electron momentum scattering. In equilibrium, the average over A is obviously zero for the rotationally symmetric fields $\mathbf{B}_{D,1}(\mathbf{k})$ and $\mathbf{B}_{D,3}(\mathbf{k})$. However, if the 2DEG is exposed to an in-plane electric field $\mathbf{E}$, the spin-polarized states are shifted from the equilibrium position in the direction of the drift wave vector $\delta\mathbf{k}=(\delta k_x,\delta k_y)=-\mu\mathbf{E}m^*/\hbar$ [Fig. 2(b)]. Note that $\mathbf{E}$ points in the opposite direction than $\delta\mathbf{k}$ because the electron mobility μ is positive by definition and $\delta\mathbf{k}$ corresponds to electrons with a negative charge. Using polar coordinates $\mathbf{k}=[r\cos(\xi),r\sin(\xi)]$, the average over the shifted area A is given by the integral

$$\mathbf{B}_{\mathrm{df,D}}(\delta\mathbf{k})=\frac{1}{A}\int_{k_{F,\downarrow}}^{k_{F,\uparrow}} rdr\int_0^{2\pi} d\xi[\mathbf{B}_D(\mathbf{k}+\delta\mathbf{k})+\mathbf{B}_S(\mathbf{k}+\delta\mathbf{k})]$$
$$=\frac{2\gamma\left[-\langle k_z^2\rangle+\frac{1}{4}(k_{F,\downarrow}^2+k_{F,\uparrow}^2)\right]+2\beta_S}{g\mu_B}\begin{pmatrix}\delta k_x\\-\delta k_y\end{pmatrix}+\mathcal{O}(\delta k^3). \quad (8)$$

This averaging transforms $\mathbf{B}_D(\mathbf{k})$ and $\mathbf{B}_S(\mathbf{k})$ into a drift field $\mathbf{B}_{\mathrm{df,D}}(\delta\mathbf{k})$ that expresses the average field experienced by the polarized electron spins. The dominant term in $\mathbf{B}_{\mathrm{df,D}}$ is linear in $\delta\mathbf{k}$, and third-order terms in $\delta\mathbf{k}$ are unimportant for $\delta k^2 \ll \langle k_z^2\rangle$ and $\delta k^2 \ll k_F^2$. We note that the terms proportional to $k_{F,\uparrow}^2$ and $k_{F,\downarrow}^2$ originate from $\mathbf{B}_{D,3}$, i.e., the cubic Dresselhaus term affects $\mathbf{B}_{\mathrm{df,D}}$ in linear order. The symmetry of $\mathbf{B}_{\mathrm{df,D}}$ is the same as that of $\mathbf{B}_{D,1}$, and the cubic terms $\mathbf{B}_{D,3}$ do change neither this symmetry nor the linearity in $\delta\mathbf{k}$. For small spin polarization, we can approximate $k_{F,\uparrow}$ and $k_{F,\downarrow}$ in Eq. (8) by the Fermi wave number k_F of the unpolarized spins. In a previous publication the influence of the cubic Dresselhaus term has been underestimated by a factor of 2 because of the assumption of a high spin polarization.[16] Using the above described simplification, reasonable for a typical experiment, we define the drift-field Dresselhaus coefficient

$$\beta^* := \gamma\left(-\langle k_z^2\rangle+\frac{1}{2}k_F^2\right)+\beta_S. \quad (9)$$

We rewrite the dominant term of Eq. (8),

$$\mathbf{B}_{\mathrm{df,D}}(\delta k_x,\delta k_y)=\frac{2\beta^*}{g\mu_B}\begin{pmatrix}\delta k_x\\-\delta k_y\end{pmatrix}. \quad (10)$$

The importance of Eq. (10) is based on the direct experimental accessibility of β^*, whereas the parameter $\beta=-\gamma\langle k_z^2\rangle$ has to be calculated from β^*, $\langle k_z^2\rangle$, k_F^2, and β_S. Temperature broadening leads to an increase of the cubic Dresselhaus contribution in Eq. (9) that becomes significant if E_F is comparable to k_BT.[27] In our measurements this correction is below 10%.

III. MEASUREMENT OF THE DRESSELHAUS SOI

We investigate Si-doped n-type material systems, namely, epitaxially grown GaAs/AlGaAs QWs and InGaAs/GaAs QWs. All QWs have been grown along [001]. The InGaAs/GaAs QWs are single QWs, whereas the GaAs/AlGaAs samples consist of a series of 14 equivalent QWs. Narrow GaAs/AlGaAs QWs are suited for a reliable determination of the Dresselhaus coupling constant γ, because GaAs/AlGaAs is a nearly strain-free system, and cubic contribution are small for narrow QWs. InGaAs/GaAs QWs with less confinement and large electron density are used to study cubic Dresselhaus SOI and to test the consistency with a strain-induced contribution. Table I summarizes the parameters of all QWs that were used.

All optical measurements have been done at elevated temperature of 40 K, to preclude nuclear spin effects. The sheet carrier density n_s of the 2DEGs was measured separately in a perpendicular magnetic field, using both Hall and Shubnikov-de Haas measurements. Both methods yield equivalent n_s at 1.6 K. The mobility was then calculated from the four-terminal resistance. A quantity that cannot be accessed in the experiment is $\langle k_z^2\rangle$. In previous publications, $\langle k_z^2\rangle\approx(\pi/w)^2$ was used, where w is the width of the QW.[12,16] This approximation is based on a square potential QW with an infinitely high confinement potential in the z direction. Note that this is an appropriate estimate only for QWs with a very large conduction-band offset. To improve the accuracy of the experimentally determined value for γ, we have used a one-dimensional Poisson and Schrödinger equation solver[28] to calculate the envelope wave function of the ground state $\psi(z)$, and then numerically determined the expectation value

$\langle k_z^2\rangle := \int[\psi'(z)]^2 dz$. The numerical approach yields $\langle k_z^2\rangle = 2.5 \times 10^{16}$ m^{-2} for a 15-nm-broad GaAs/$Al_{.3}Ga_{.7}As$ QW. This is considerably less than for an infinite barrier $[(\pi/15\ \text{nm})^2 = 4.4\times 10^{16}\ \text{m}^{-2}]$ because of leakage of the wave function into the barrier region and electron screening.

To apply an in-plane electric drift field **E** in a specific direction, a mesa structure is etched into the substrates hosting the 2DEG to form 100-μm-wide or 150-μm-wide conductive channels. The geometry of the mesa structure is cross shaped for samples 1 and 3, whereas unidirectional mesa bars were used for the other samples. The electric field is inhomogeneous in the center of the cross-shaped mesa, a fact that has been accounted for in the evaluation.[16] Ohmic contacts to the buried channel are subsequently fabricated by standard AuGe diffusion. In the experiment, a small spin polarization of the electron spins in the conduction band of the QW is generated by a circularly polarized pump pulse generated by a mode-locked Ti:sapphire laser. The energy per area of the pump pulses was kept below 2×10^{-2} J m^{-2} for sample 1 and 2, and below 4×10^{-3} J m^{-2} for samples 3–5. These small intensities ensure that the number of electron-hole pairs that are excited per QW is much smaller than the number of electrons already in the QW. Therefore, only a small fraction of the electrons become spin polarized by the pump pulse.

The experiment then monitors, in the time domain, the coherent precession of electron spins in an external magnetic field $\mathbf{B}_{\text{ext}}$ using time-resolved Kerr rotation (TRKR) or time-resolved Faraday rotation (TRFR).[15] The spin-precession frequency is given by

$$\Omega(\mathbf{E}) = \frac{|g|\mu_B}{\hbar}|\mathbf{B}_{\text{ext}} + \mathbf{B}_{\text{df}}(\mathbf{E})|. \tag{11}$$

$\mathbf{B}_{\text{ext}}$ is applied in the plane of the QW, and SOI-induced contributions to the spin splitting become visible as an **E**-field-dependent change in Ω given by $\Delta\Omega(\mathbf{E}) = \Omega(\mathbf{E}) - \Omega(0)$. The observation of several periods of spin precession during the spin lifetime is required to precisely determine Ω and thus $\Delta\Omega$. This is made possible by exposing the sample to $\mathbf{B}_{\text{ext}} \approx 1$ T. In bulk GaAs, where the spin lifetime is much longer than in QWs, coherent spin precession about $\mathbf{B}_{\text{df}}$ has been observed at $\mathbf{B}_{\text{ext}} = 0$ T.[14]

For our experiments, $|\mathbf{B}_{\text{df}}| \ll |\mathbf{B}_{\text{ext}}|$, and therefore $\Delta\Omega$ can be approximated by

$$\Delta\Omega(\mathbf{E}) \approx \frac{|g|\mu_B}{\hbar}\frac{\mathbf{B}_{\text{df}}(\mathbf{E})\cdot\mathbf{B}_{\text{ext}}}{|\mathbf{B}_{\text{ext}}|}, \tag{12}$$

i.e., $\Delta\Omega$ is proportional to the projection of $\mathbf{B}_{\text{df}}$ along the direction of the external field. By selecting the orientation of $\mathbf{B}_{\text{ext}}$ with respect to **E**, the contributions with Dresselhaus symmetry, $\Delta\Omega_D$, can be separated from contributions having another symmetry. We used two different methods for this separation,

(I) $\mathbf{E} \perp \mathbf{B}_{\text{ext}}$ with $\mathbf{B}_{\text{ext}} \parallel [1\bar{1}0]$ or $[110]$,

(II) $\mathbf{E} \parallel \mathbf{B}_{\text{ext}}$ with $\mathbf{B}_{\text{ext}} \parallel [100]$ or $[010]$.

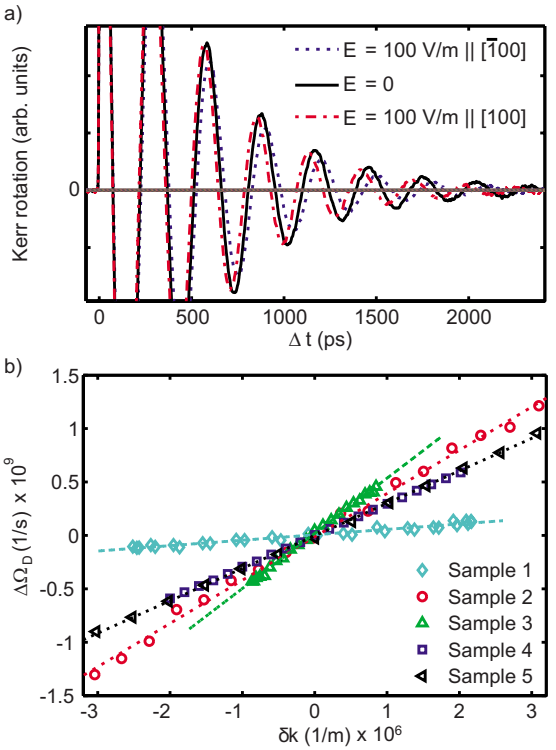

FIG. 3. (Color online) (a) TRKR measurements as a function of the electric drift-field E (sample 4, $\mathbf{B}_{\text{ext}}$ along [100], $|\mathbf{B}_{\text{ext}}| = 0.93$ T). (b) The Dresselhaus drift-induced frequency shift $\Delta\Omega_D$ depends linearly on the drift wave vector δk for all samples measured.

For (I), $\Delta\Omega(\mathbf{E})$ is recorded for two orientations of $\mathbf{B}_{\text{ext}}$,[29] and the sum of these two measurements yields the Dresselhaus contribution $\Delta\Omega_D$.[15] For (II), $\Delta\Omega$ is a direct measure of the Dresselhaus contribution $\Delta\Omega_D$,[15,30] i.e.,

$$\Delta\Omega(\mathbf{E}) = \Delta\Omega_D(\mathbf{E}) \approx \pm\frac{|g|\mu_B}{\hbar}|\mathbf{B}_{\text{df,D}}(\mathbf{E})|. \tag{13}$$

As an example, data from sample 4 are shown where we used method II to directly see the influence of the Dresselhaus SOI. Figure 3(a) shows experimental TRKR traces measured with $\mathbf{B}_{\text{ext}} = 0.93$ T applied along [100]. The g factor $|g|$ is obtained from the trace at $E = 0$. Also the data for **E** along $[\bar{1}00]$ and **E** along [100] have been plotted. In this configuration, Ω increases for **E** along [100].

As a central finding, we show that $\Delta\Omega_D$ depends linearly on the drift wave number δk [Fig. 3(b)]. This is supported by experimental data from various samples (listed in Table I). For samples 1 and 2, $\Delta\Omega_D$ has been obtained using method (I), and for samples 3–5, we used method (II). According to Eqs. (10) and (13), the slope of the fit in Fig. 3(b) is given by $2\beta^*/\hbar$. The sign of β^* is determined from the direction of $\mathbf{B}_{\text{df,D}}$ with respect to $\mathbf{B}_{\text{ext}}$: for example, for **E** along $[\bar{1}00]$ $(=-\hat{x})$, $\delta\mathbf{k}$ points along [100] and, according to Eq. (10), $\mathbf{B}_{\text{df,D}}$ points along $[\bar{1}00]$ for $\beta^* > 0$ and $g < 0$. From Eq. (12), we see that $\Delta\Omega_D$ is negative if $\mathbf{B}_{\text{ext}}$ is applied along [100]. Therefore, the sign of β^* must be positive for the data shown

in Fig. 3(a). As seen from Table I, we find $\beta^* > 0$ for all samples investigated.

IV. DISCUSSION

First, we will discuss the results for GaAs/AlGaAs and compare $|\gamma|$ with the literature values. Second, we present the results for InGaAs/GaAs, for which we expect a significant contribution to SOI from third-order terms and strain. Finally, we compare the sign of γ we obtained with the results of other experimental work.

As GaAs/AlGaAs grows nearly strain free, we assume $\beta_S = 0$ and calculate γ directly from the measured β^* using Eq. (9) and the values of $\langle k_z^2 \rangle$ and k_F^2 (Table I). For γ, we find values in the range of -4 to -8 eV Å^3. These values are smaller than previously reported for GaAs/AlGaAs QWs (Refs. 7–9 and 31) and GaAs bulk crystals,[11] where $|\gamma|$ covers a rather wide range of 11–27 eV Å^3. Recent results from spin-grating measurements yield $|\gamma| = 5$ eV Å^3, assuming $\langle k_z^2 \rangle = (\pi/w)^2 = 6.8 \times 10^{16}$ m^{-2}.[12] For these QWs, our simulations suggest $\langle k_z^2 \rangle = 3.4 \times 10^{16}$ m^{-2}, which corresponds to $|\gamma| = 10$ eV Å^3. A similar result of $|\gamma| \approx 8$ eV Å^3 was found for a quantum dot hosted in an AlGaAs/GaAs heterostructure.[10] Measurements of spin-orbit-induced spin precession at $B_{ext} = 0$[32] and of g anisotropy[33] yields values of $|\gamma|$ between 4 and 10 eV Å^3. Results from theoretical calculations are in the range of $|\gamma| = 8$–36 eV Å^3 (see supplementary notes of Ref. 10).

There are several possibilities for an error in the experimental value for γ. In particular, a systematic underestimation of γ could result from a reduction in the drift wave number δk under optical illumination. The electric field E and therefore δk have been determined from the four-terminal resistance measured simultaneously with the TRKR (TRFR). The pump pulse locally creates electron-hole pairs that initially screen the applied electric field. This effect can be reduced by using pump pulses with smaller intensities. Indeed, we observe a small dependence of β^* upon the pump power. For sample 5, β^* increases to about 1.2×10^{-13} eV m if the pump intensity is decreased by a factor of 8 (reaching 5×10^{-4} J m^{-2}). We have not observed a persistent photoeffect: the average electron density as determined from both Hall and Shubnikov-de Haas measurements did not change significantly upon illumination with a light-emitting diode.

To investigate the effect of cubic Dresselhaus SOI and to quantify the importance of cubic terms compared with that of linear terms, we have chosen samples with large n_s and small $\langle k_z^2 \rangle$, such that $k_F^2 \gtrsim 2\langle k_z^2 \rangle$ (sample 1). For this sample, we find $\beta^* > 0$, which at first sight is surprising because β^* is expected to change sign for $k_F^2 > 2\langle k_z^2 \rangle$ if $\beta_S = 0$ [Eq. (9)]. The positive sign can be explained if strain affects the SOI. For simplicity, we assume that samples 1 and 2 have the same γ and β_S. With the values of β^*, $\langle k_z^2 \rangle$, and k_F^2 listed in Table I, we solve the set of equations given by Eq. (9) with the two unknowns β_S and γ. As a result we obtain $\beta_S \approx 7 \times 10^{-14}$ eV m and $\gamma \approx -7.5$ eV Å^3. This value for γ is in rather good agreement with the results for the GaAs/AlGaAs QWs and suggests that 2D structures can exhibit strain-induced spin splitting with magnitudes comparable to the linear Dresselhaus SOI ($\beta_S \approx \beta \approx 7 \times 10^{-14}$ eV m for sample 1). In this analysis, the biaxial strain component directly affects the resulting β^*, and further more systematic investigations are needed to obtain a more precise value for γ in InGaAs/GaAs QWs.

In our measurements, the sign of γ is negative for all samples. Some care has to be taken to determine the sign of γ. We have experimentally verified the sign of the magnetic field in our laboratory. Moreover, the sign is based on the assumption that $g < 0$ and that the drift direction is the opposite direction of $\mathbf{E}$, i.e., $\delta\mathbf{k} \| -\mathbf{E}$. We have kept track of the crystallographic direction indicated by the wafer manufacturer during processing and double checked with a selective etching test.[21,22] The often cited positive sign of γ is specified in an As-based coordinate system, which translates to a negative sign in a Ga-based system.[23]

In Ref. 34 the sign of γ for a GaAs bulk crystal has been measured by analyzing the phase that an electron spin acquires during traveling. A positive γ has been obtained in an As-based coordinate system, in agreement with our result. The sign of γ can also be compared with experiments that only determine the sign of the ratio α/β if the sign of α is known. From previous measurements on a parabolic QW with back and front gates,[35] the sign of α has been determined to be positive for an electric field $\mathbf{E}_\perp$ pointing along the growth direction $(+\mathbf{z}) \| [001]$. From $\beta = -\gamma \langle k_z^2 \rangle > 0$, it follows that α/β is positive for $\mathbf{E}_\perp \| (+\mathbf{z})$. This is in agreement with Ref. 36: using a ballistic spin resonance experiment, a negative sign of α/β has been determined in the heterostructure investigated with $\mathbf{E}_\perp$ along $-\hat{\mathbf{z}}$. It is also compatible with Ref. 37: α/β is determined from the spin-dephasing anisotropy and becomes negative for bias voltages larger than 1.2 V. In that experiment, β is defined as $+\gamma \langle k_z^2 \rangle$ ($= -\beta$ in our definition), and a positive bias means a negative voltage on the front gate and ground potential on the back gate, i.e., $\mathbf{E}_\perp$ is along $+\hat{\mathbf{z}}$.[38]

To summarize, we have shown how SOI in 2DEGs manifests itself in drift-related experiments: the drift-induced spin splitting due to Dresselhaus SOI is linear in the drift velocity given by the drift wave number. The linear proportionality is characterized by β^*. Cubic Dresselhaus SOI becomes important for a large electron density and weak electron confinement, and lowers the value of β^* by a factor of $1 - \frac{1}{2} k_F^2 / \langle k_z^2 \rangle$. Already in a 15-nm-wide GaAs/$Al_{.3}Ga_{.7}As$ QW with an electron density of 1.6×10^{15} m^{-2}, β^* is reduced by 20% compared with $\beta = -\gamma \langle k_z^2 \rangle$. We have experimentally determined β^* from the drift-induced change in the spin-precession frequency. The Dresselhaus coupling constant γ was obtained from the β^* measured, using the electron density from Hall measurements and the simulation result for $\langle k_z^2 \rangle$. For GaAs/AlGaAs QWs, we find $\gamma \approx -6$ eV Å^3, and for an InGaAs/GaAs QWs, $\gamma \approx -8$ eV Å^3. The results for InGaAs/GaAs QWs underline the importance of cubic Dresselhaus SOI, and provide evidence of a significant contribution from biaxial strain. The negative sign of γ agrees with theoretical work, and is compatible with various experimental results for α/β, assuming α to be positive for electrons that are pushed toward the substrate by the structure inversion asymmetry of the quantum well.

ACKNOWLEDGMENTS

We thank M. Cardona, J. A. Folk, and S. D. Ganichev for discussions and would like to acknowledge financial supported from the KTI and the NCCR Nano.

*Author to whom correspondence should be addressed; gsa@zurich.ibm.com

[1] S. Datta and B. Das, Appl. Phys. Lett. **56**, 665 (1990).
[2] D. Loss and D. P. DiVincenzo, Phys. Rev. A **57**, 120 (1998).
[3] S. A. Wolf, D. D. Awschalom, R. A. Buhrman, J. M. Daughton, S. von Molnar, M. L. Roukes, A. Y. Chtchelkanova, and D. M. Treger, Science **294**, 1488 (2001).
[4] Y. A. Bychkov and E. I. Rashba, J. Phys. C **17**, 6039 (1984).
[5] G. Dresselhaus, Phys. Rev. **100**, 580 (1955).
[6] M. I. Dyakonov and V. Y. Kachorovskii, Sov. Phys. Semicond. **20**, 110 (1986).
[7] B. Jusserand, D. Richards, H. Peric, and B. Etienne, Phys. Rev. Lett. **69**, 848 (1992).
[8] P. D. Dresselhaus, C. M. A. Papavassiliou, R. G. Wheeler, and R. N. Sacks, Phys. Rev. Lett. **68**, 106 (1992).
[9] J. B. Miller, D. M. Zumbühl, C. M. Marcus, Y. B. Lyanda-Geller, D. Goldhaber-Gordon, K. Campman, and A. C. Gossard, Phys. Rev. Lett. **90**, 076807 (2003).
[10] J. J. Krich and B. I. Halperin, Phys. Rev. Lett. **98**, 226802 (2007).
[11] V. A. Maruschak, M. N. Stepanova, and A. N. Titkov, Sov. Phys. Solid State **25**, 2035 (1983).
[12] J. D. Koralek, C. P. Weber, J. Orenstein, B. A. Bernevig, S.-C. Zhang, S. Mack, and D. D. Awschalom, Nature (London) **458**, 610 (2009).
[13] V. K. Kalevich and V. L. Korenev, JETP Lett. **52**, 230 (1990).
[14] Y. Kato, R. C. Myers, A. C. Gossard, and D. D. Awschalom, Nature (London) **427**, 50 (2004).
[15] L. Meier, G. Salis, I. Shorubalko, E. Gini, S. Schön, and K. Ensslin, Nat. Phys. **3**, 650 (2007).
[16] M. Studer, S. Schön, K. Ensslin, and G. Salis, Phys. Rev. B **79**, 045302 (2009).
[17] Z. Wilamowski, H. Malissa, F. Schäffler, and W. Jantsch, Phys. Rev. Lett. **98**, 187203 (2007).
[18] A. Chernyshov, M. Overby, X. Liu, J. K. Furdyna, Y. Lyanda-Geller, and L. P. Rokhinson, Nat. Phys. **5**, 656 (2009).
[19] B. M. Norman, C. J. Trowbridge, J. Stephens, A. C. Gossard, D. D. Awschalom, and V. Sih, Phys. Rev. B **82**, 081304(R) (2010).
[20] B. A. Bernevig and S.-C. Zhang, Phys. Rev. B **72**, 115204 (2005).
[21] D. W. Shaw, J. Electrochem. Soc. **128**, 874 (1981).
[22] S. Adachi and K. Oe, J. Electrochem. Soc. **130**, 2427 (1983).
[23] M. Cardona, N. E. Christensen, M. Dobrowolska, J. K. Furdyna, and S. Rodriguez, Solid State Commun. **60**, 17 (1986).
[24] M. Cardona, N. E. Christensen, and G. Fasol, Phys. Rev. B **38**, 1806 (1988).
[25] F. Meier and B. Zakharchenya, *Optical Orientation* (North-Holland, New York, 1984).
[26] S. Studenikin, P. Coleridge, P. Poole, and A. Sachrajda, JETP Lett. **77**, 311 (2003).
[27] M. Q. Weng, M. W. Wu, and L. Jiang, Phys. Rev. B **69**, 245320 (2004).
[28] Calculations were done with the NEXTNANO3 software version August 24, 2004.
[29] $\mathbf{B}_{\mathrm{df,D}}$ and $\mathbf{B}_{\mathrm{df,R}}$ are either parallel or antiparallel for this set of directions.
[30] $\mathbf{B}_{\mathrm{df,D}} \perp \mathbf{B}_{\mathrm{df,R}}$ for this set of directions, and $\mathbf{B}_{\mathrm{df}} \cdot \mathbf{B}_{\mathrm{ext}} = \mathbf{B}_{\mathrm{df,D}} \cdot \mathbf{B}_{\mathrm{ext}}$.
[31] B. Jusserand, D. Richards, G. Allan, C. Priester, and B. Etienne, Phys. Rev. B **51**, 4707 (1995).
[32] W. J. H. Leyland, R. T. Harley, M. Henini, A. J. Shields, I. Farrar, and D. A. Ritchie, Phys. Rev. B **76**, 195305 (2007).
[33] P. S. Eldridge, J. Hübner, S. Oertel, R. T. Harley, M. Henini, and M. Oestreich, arXiv:1010.2142.
[34] H. Riechert, S. F. Alvarado, A. N. Titkov, and V. I. Safarov, Phys. Rev. Lett. **52**, 2297 (1984).
[35] M. Studer, G. Salis, K. Ensslin, D. C. Driscoll, and A. C. Gossard, Phys. Rev. Lett. **103**, 027201 (2009).
[36] S. M. Frolov, S. Lüscher, W. Yu, Y. Ren, J. A. Folk, and W. Wegscheider, Nature (London) **458**, 868 (2009).
[37] A. V. Larionov and L. E. Golub, Phys. Rev. B **78**, 033302 (2008).
[38] L. E. Golub (private comunication).